Check for
updates

Interband transitions and exciton binding energy in a Razavy quantum well: effects of external fields and Razavy potential parameters

M. Sayrac[1,a] ⓘ **, A. John Peter**[2]**, F. Ungan**[3]

[1] Department of Nanotechnology, Faculty of Engineering, Sivas Cumhuriyet University, 58140 Sivas, Turkey
[2] P.G and Research Department of Physics, Government Arts College, Melur, Madurai 625 106, India
[3] Department of Physics, Faculty of Science, Sivas Cumhuriyet University, 58140 Sivas, Turkey

Abstract In this paper, we theoretically investigated the influence of externally applied fields such as high-frequency non-resonant intense laser fields, static electric and magnetic fields, as well as structure parameters, on the interband transitions and exciton binding energy of a GaAs quantum well with Razavy confinement potential. To perform numerical calculations, the ground state electron and heavy hole subband energy levels of the structure and the envelope wave functions corresponding to these states were calculated using a variational method within the framework of the effective mass and parabolic band approaches. After obtaining the numerical values, the band transitions of the structure, the exciton binding energy, the dipole moment matrix elements, and the transition energy between the ground state electron and heavy hole subband energies of the structure were evaluated in detail. The results show that the Razavy potential profile turns into a single QW structure for particular dimensionless structure parameters and the peak position of the interband transition coefficient shifts toward red (lower energy) with the increase in the structure parameters and electric field strength, while it shifts toward the blue (higher energy) with the increase in the intensity of the intense laser field and magnetic field. We believe that these numerical results will be useful in the design and production of next-generation electronic and optoelectronic devices.

1 Introduction

Recent development in semiconductor structures such as quantum wells (QWs), quantum dots, and quantum-well wires have caught huge attention for designing and fabricating low- dimensional semiconductor devices. In the design of new generation optoelectronic devices connected to semiconductor structures, it is necessary to choose the structure parameters correctly by considering many factors such as the confinement potential geometry, doped layers, and structure dimensions. In addition to these structural parameters, the interaction of the examined system with applied external perturbations such as electric field, magnetic field, hydrostatic pressure, temperature, and non-resonant intense laser field (*ILF*) should also be considered. All these factors have a critical role in tuning the optical and electronic properties of the structure [1–13]. It is expected that the application of an external field, i.e., electric field (or magnetic field), modifies the potential profile and the corresponding wavefunctions are relocated toward to edge (or center) of the structure. This modification produces a reasonable change in the subband energy levels, the transition energies, and the optical absorption coefficient of the structure. Theoretical and experimental studies have been performed by considering the effect of the influence of external fields [14–24]. Dakhlaoui et al. [25] explored the red and blue shifts of the total optical absorption coefficients (TOAC) in double GaAs heterostructures. Optical properties of hyperbolic QW exposed to the electric and magnetic field were reported by Ungan et al. [26]. Hien et al. [27] discussed the magneto-optical properties, which were affected by the applied external fields.

In addition to the applied external fields, the doping technique is another concept in semiconductor processing [28–36]. The doping method is practical to adjust the optical and electronic properties of the structure. For example, the δ doping technique is done by inserting thin layer silicon atoms in GaAs-based structures. Moreover, the silicon layer doping introduces a triangular QW, and this doping layer affects the spread of the wavefunctions [37–40]. The experimental and theoretical research explored the effect of doping on the total optical absorption coefficients (TOAC) in the semiconductor quantum nanostructures [41–45]. Gaggero-Sager et al. [46] investigated the temperature effect on the energy levels in a single doped QW. Dhafer et al. [25] explored that the inserted doping layer improves the amplitude of the optical gain that is critical for fiber optical communications [47]. Razavy [48] explored the quantum theory of molecules described by considering the motion of a particle taking the effects of two force fields. After that exploration, these types of potentials are called Razavy potentials [49, 50]. The effect of an intense laser field on the TOAC coefficient was studied in Ref. [51].

[a] e-mail: muhammedsayrac@cumhuriyet.edu.tr (corresponding author)

Quantum wires (QWRs) are another type of heterostructures, in which electrons are confined in the transverse plane, i.e., therefore they can move in one dimension. For this reason, the energy levels of such structures present a discrete spectrum. QWRs have been studied for more than four decades [52–54]. As the above references, these kinds of low dimensional structures find broad applications in semiconductor devices such as transistors and efficient solar cells [55]. For this reason, improvement in the electronic and optical properties is a must for developing highly efficient structures. To achieve this aim, there are several studies have been conducted recently [56–58].

From the above-mentioned references, the nonlinear optical properties of QWs structures were based on the electronic state transitions. Exciton effects in QW structures are other parameters that have crucial importance in tuning nonlinear optical properties. The excitonic transitions are important for determining the optical properties of the heterostructure [37–39] and provide valuable information about the quality of the heterostructure [40]. These exciton effects in the QW structure introduce a noticeable boost in the optical absorption coefficients and refractive index changes. Therefore, an investigation of the excitonic effects on the nonlinear optical properties of the structure would be interesting.

As known, the variation of structure parameters and applied external fields modify the respective electron and heavy hole subband energy levels and their corresponding wave functions which directly affect the electronic and optical properties of GaAs QW with Razavy confining potential. To reach this aim, in this study, the influence of structure parameters and applied external fields on the interband transitions and exciton binding energy in GaAs QW with Razavy confinement potential are investigated in detail for the first time. The obtained numerical results for exciton binding energy and interband transition coefficients are presented for different structural parameters and different magnitudes of externally applied electric, magnetic, and non-resonant *ILF*.

This paper is organized as follows: Sect. 2 gives theoretical background. The discussion and numerical solutions are given in Sect. 3. Finally, the conclusion is presented in Sect. 4.

2 Theory

In the present work, we consider a GaAs QW structure with Razavy potential grown along the z-direction. The schematic representation of the structure is shown in Fig. 1 We aim to examine the effect of externally applied fields and structural parameters on the exciton binding energy and exciton absorption coefficient of this structure. For this purpose, the static electric field ($\boldsymbol{F} = F\widehat{z}$) along the z-axis, and a static magnetic field ($\boldsymbol{B} = B\widehat{x}$) along the x-axis and a non-resonant high-frequency intense laser field with polarization parallel to the z-axis were applied to the structure. Moreover, the quantum wells with different confining potentials were obtained by changing the structural parameters such as A and M of the system.

The Hamiltonian for the electron–hole pair in GaAs QW with Razavy potential in the presence of only the static electric and the magnetic field is given by

$$
\begin{aligned}
H = {} & \frac{1}{2m_e}\left(\boldsymbol{P}_e + \frac{e}{c}A(\boldsymbol{r}_e)\right)^2 + V_R(z_e) \\
& - eFz_e + \frac{1}{2m_h}\left(\boldsymbol{P}_h - \frac{e}{c}A(\boldsymbol{r}_h)\right)^2 \\
& + V_R(z_h) + eFz_h - \frac{e^2}{\varepsilon_0|\boldsymbol{r}_e - \boldsymbol{r}_h|},
\end{aligned}
\tag{1}
$$

where the mass of the electron (hole) is $m_{e(h)}$, and e, the elementary charge, ε_0, dielectric constant, and c, speed of light are universal constants. The electron (hole) momentum operator is $\boldsymbol{P}_{e(h)}$, $A = (0, -Bz, 0)$ is the vector potential of the static magnetic field, F is the strength of the applied static electric field, $\boldsymbol{r}_{e(h)}$ is the electron (hole) position. In the absence of non-resonant *ILF*, the confinement potential profile of electrons (holes) in the z-direction ($V_R(z_{e(h)})$) is given by the following expression [51]

$$
V_R\big(z_{e(h)}\big) = V_0^{e(h)}\left[A\cosh\left(\frac{z}{\eta}\right) - M\right]^2
\tag{2}
$$

where $V_0^{e(h)}$ is the conduction (valance) band offset, A and M are the dimensionless structure parameters, and η is the QW width.

$\boldsymbol{R} = (m_e\boldsymbol{r}_e + m_h\boldsymbol{r}_h)/(m_e + m_h)$ is the center of mass coordinate, and $\boldsymbol{r} = (\boldsymbol{r}_e - \boldsymbol{r}_h)$ is the relative coordinate. For the constant motion of the center of mass, the Hamiltonian of the system using the cylindrical coordinates ($x = \rho cos\phi$, $y = \rho sin\phi$, $z = z$) as follows [59].

$$
\begin{aligned}
H = {} & -\frac{\hbar^2}{2\mu}\left(\frac{\partial^2}{\partial\rho^2} + \frac{1}{\rho}\frac{\partial}{\partial\rho} + \frac{1}{\rho^2}\frac{\partial^2}{\partial\phi^2}\right) \\
& - \frac{\hbar^2}{2m_e}\frac{\partial^2}{\partial z_e^2} - \frac{\hbar^2}{2m_h}\frac{\partial^2}{\partial z_h^2} \\
& - \frac{eB}{c}\left(\frac{z_e}{m_e} + \frac{z_h}{m_h}\right)P_y + \frac{e^2 B^2}{2m_e c^2}z_e^2
\end{aligned}
$$

Fig. 1 Schematic representation of GaAs Razavy quantum well system in the absence of external perturbations
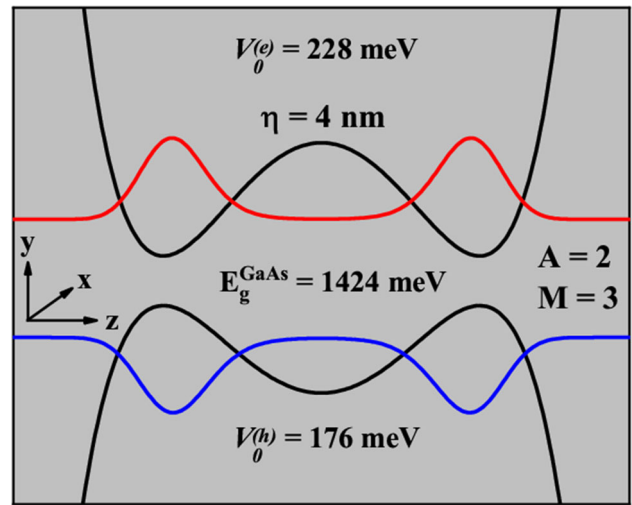
$$+ \frac{e^2 B^2}{2 m_h c^2} z_h^2 - \frac{e^2}{\varepsilon_0 \sqrt{\rho^2 + (z_e - z_h)^2}} + V_R(z_e)$$
$$+ V_R(z_h) - eFz_e + eFz_h, \tag{3}$$

where μ is the reduced mass, $\mu = m_e m_h / (m_e + m_h)$, $\rho = \sqrt{(x_e - x_h)^2 + (y_e - y_h)^2}$ is the relative distance between the electron and hole in the $(x - y)$ plane. The expectation value of the third term- $\frac{eB}{c}\left(\frac{z_e}{m_e} + \frac{z_h}{m_h}\right) P_y$- in the Hamiltonian, is zero according to the selected trial wave function in Eq. (6).

The non-resonant intense laser field on the structure distorts the confinement potential. After the *ILF* is applied to the structure, the new-formed confinement potential is called "dressed" confinement potential [51].

$$V_R\big(z_{e(h)}\big), \alpha_0\big) = \frac{\varpi}{2\pi} \int_0^{\frac{2\pi}{\varpi}} V_R\big(z_{e(h)} + \alpha_0 \sin\varpi t\big) dt \tag{4}$$

here ϖ is the non-resonant laser frequency, $\alpha_0 = \frac{q A_0}{m_{e(h)} \varpi^2}$ is the laser dressing parameter, A_0 is the laser field strength. In addition to the confinement potential, the *ILF* also affects the Coulomb potential. The new-formed Coulomb potential is written as [60]

$$V_C\big(z_{e(h)}, \alpha_0\big) = -\frac{e^2}{2\varepsilon_0}\left[\frac{1}{\sqrt{\rho^2 + (z_e + \alpha_0 - z_h)^2}} + \frac{1}{\sqrt{\rho^2 + (z_e - \alpha_0 - z_h)^2}}\right]. \tag{5}$$

The trial wave function for the electron–hole system is chosen as

$$\Phi(\rho, \phi, z_e, z_h, \xi, \kappa) = N \psi(z_e) \psi(z_h) \exp\left[-\sqrt{\frac{\rho^2}{\xi^2} + \frac{(z_e - z_h)^2}{\kappa^2}}\right], \tag{6}$$

where N is the normalization constant, ξ and κ are the variational parameters, $\psi(z_e)$ and $\psi(z_h)$ represent the motions of the electron and hole in the z-axis.

Using Eq. 6, the time-independent Schrödinger equation for the excitonic structure is expressed as

$$H\Phi(\rho, \phi, z_e, z_h, \xi, \kappa) = E\Phi(\rho, \phi, z_e, z_h, \xi, \kappa) \tag{7}$$

where E is the total energy of the system.

Using a variational method, the exciton binding energy is obtained as

$$E_b = E_{z_e} + E_{z_h} - \min_{\xi, \kappa} \underbrace{\langle \psi | H | \psi \rangle} \tag{8}$$

where $E_{z_e}(E_{1e})$ and $E_{z_h}(E_{1h})$ are the electron and hole first subband energies, respectively.

The general expression for the optical absorption coefficient in the compact-density matrix approach is given by [61, 62]

$$\beta(\omega) = \omega \sqrt{\frac{\mu}{\varepsilon_0}} \frac{|M_{12}|^2 \sigma_v \hbar \Gamma_{12}}{\left(E_{1e} + E_{1h} + E_g^{GaAs} - E_b - \hbar\omega\right)^2 + (\hbar\Gamma_{12})^2} \tag{9}$$

Fig. 2 Razavy QW potential shape and corresponding wave functions as a function of different dimensionless A and M parameters **a** at constant $M = 3$ and **b** at constant $A = 2$
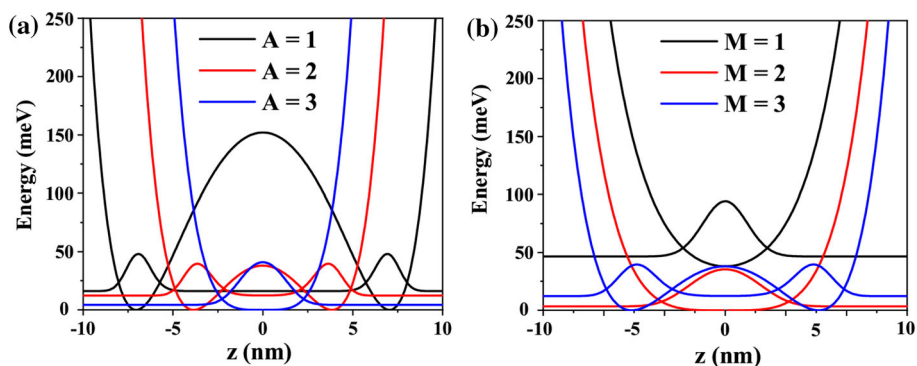
where ω is the angular frequency of the incident photon, μ is the permeability, σ_v is the electron density in the structure, $\hbar$ is reduced Planck's constant, $M_{12} = \psi_i(z_e)|ez|\psi_f(z_h)$, and $\Gamma_{12} = \frac{1}{\tau_{12}}$ is the inverse of interband relaxation time.

3 Results and discussion

In this section, we present our results of numerical simulations on GaAs QW with Razavy potential. We firstly obtained the effects of structure parameters (A, M, and η) and the applied external static electric field (F), magnetic field (B), and a non-resonant *ILF* (α_0) on the exciton binding energy, the off-diagonal electric dipole moment matrix elements, and the interband transition energy of the structure. Then, we investigated the effect of these external fields and structural parameters on the optical absorption coefficient of the system. The numerical simulation is performed in three consecutive steps; (*i*) the single parabolic band and effective-mass approaches are applied to obtain the energy eigenvalues and eigenfunctions of ground state electron and heavy hole, (*ii*) the variational calculation technique was used to compute the exciton binding energy and (*iii*) the optical interband absorption coefficients are calculated by using the compact-density matrix approach. The physical constant used for the numerical calculation are follows [63]: $V_0^e = 228$ meV, $V_0^h = 176$ meV, $m_e = 0.067m_0$, $m_{hh} = 0.45m_0$, (m_0 is the free electron mass), $\sigma_v = 3 \times 10^{22}\ textm^{-3}$, $\hbar = 1.056 \times 10^{-34}$ Js $E_g^{GaAs} = 1424\ textmeV$, $e = 1.602 \times 10^{-19}$ C, $\varepsilon_0 = 8.854 \times 10^{-12}$, $n_r = 3.2$, $\varepsilon_0 = 12.58$, $\mu = 4\pi \times 10^{-7}$ Hm^{-1}, $\tau_{12} = 0.14$ ps, $I = 0.1\ MWcm^{-2}$.

Figure 1 is the demonstration of GaAs Razavy QW for an electron wave function in the conduction band and a hole in the valance band. Figure 2 compares the potential profiles at different structure parameters. In Fig. 2a, the structure parameters M sets to 3. The potential profile is double QW having reasonable barrier width at the middle for $A = 1$. For $A = 2$, the potential profile barrier width decreases. When A sets to 3, the potential profile turns into a single QW structure. Figure 2b, at constant $A = 2$, the bottom of the potential well moves upward for $M = 1$. For this reason, the wave function moves toward upper energy. At $M = 2$, the potential shape turns into a single QW structure. Finally, $M = 3$, the potential shape turns into a double QW structure. It is brought out that the quantum-well system evolves from the single quantum well to the double quantum well depending on the Razavy potential parameters.

The exciton binding energy as a function of QW width at different dimensionless parameters is given in Fig. 3. At constant $M = 3$, when the $A = 1$, the potential barrier between two QW is large (see Fig. 2a). When the A increases to $A = 2$, the barrier between two QW decreases. There is a change over from a double quantum well to a single quantum well. When the $A = 3$ the potential profile turns into a single QW structure. Figure 3a, the increment of parameter QW width (η) for constant $A = 1$ and $M = 3$ results in a change of electron energy levels of an electron occupied in the potential profile. For $A = 1$ and $M = 3$, the electron feels a double QW structure. The increment of η results in the increment of the exciton binding energy difference. $A = 2$ and $M = 3$, the structure approaches the single QW structure having small barrier width, and the exciton binding energy starts decreasing with the increment of η (QW width). $A = M = 3$, the structure has a flat well shape with an infinite potential barrier of a single QW. The increment of the potential width leads to the decrement of the exciton binding energy [42]. Figure 3b presents the variation of the exciton binding energy as a function of η at different M parameters for a constant, $A = 2$. The exciton binding energy decreases with the change of the dimensionless M parameters. The potential profile shape changes into double or single QW in which the exciton binding energy is affected. The electron wavefunction is vertically shifted for $M = 1$. It implies that the wavefunctions move toward higher energies. When M and A are equal to 2, the potential structure shifts to the origin position, and the potential width increases. When $M = 3 > A$, the coupling of two potential wells increases, resulting in the double QW [29].

The applied external fields of the electric field, magnetic field, and intense laser field modify the shape of the potential well. The bottom of the QW potential is tilted (+ z-direction) with the applied electric field, while the valance band is tilted in the opposite direction (+ z-direction). This potential distortion shifts the electron wavefunction in the conduction band and the heavy hole in the valance band in opposite directions. The confined electron and heavy hole drift in different directions. As a result, the electron and heavy hole interaction probability decreases which leads to the decrement of the exciton binding energy as shown in Fig. 4a–b. On

Fig. 3 Variation of exciton binding energy as a function of quantum well width for different structure parameters; **a** with the variation of A and **b** with the variation of M
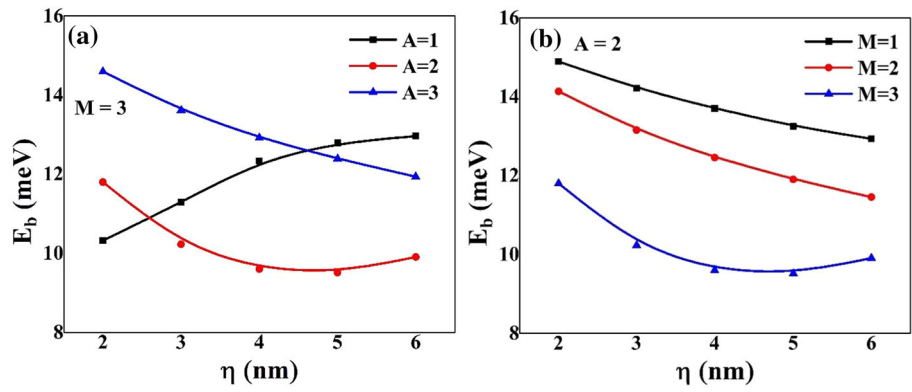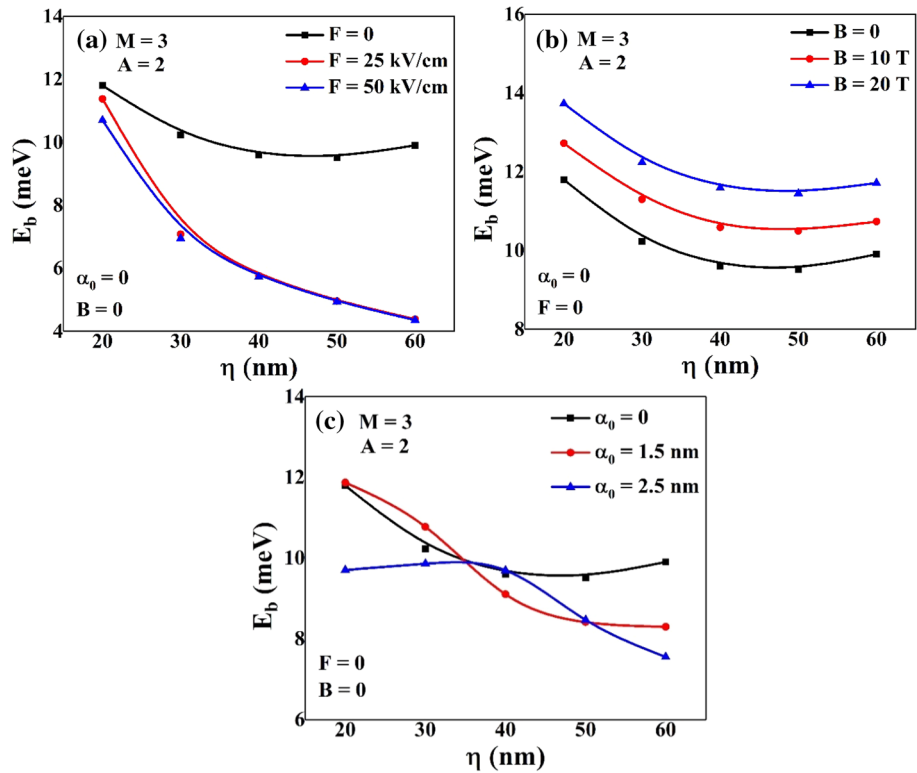

Fig. 4 Variation of exciton binding energy as a function of quantum well width for different applied external fields **a** electric field **b** magnetic field and **c** intense laser field

the other hand, the exciton binding energy does not linearly vary with the applied ILF as seen in Fig. 4c. At $\alpha = 0$, the binding energy decreases with the increment of potential width. When α is turned on, the width of the potential well narrows. Interaction of the electron and the heavy hole is more reasonable, and the exciton binding energy increases [43]. Then, the exciton binding energy decreases with the increment of the η parameter.

Interband transition energy between the electron in the conduction band and the heavy hole in the valance band is controlled with the structure parameters and the applied external fields. Figure 5a shows that the interband transition energy decreases with the increment of dimensionless A parameters. The dipole moment matrix element like a normal distribution initially increases and decreases with the increment of A. Figure 5b gives interband transition energy as a function of the M parameter. Energy difference decreases with the increment of M parameters, and the dipole moment matrix elements increase with M.

Figure 6 presents the interband energy transition as a function of applied external fields. Interband transition energy is found to change as functions of applied external electric fields. Figure 6a displays that the potential profile is modified with the applied electric field. The interband energy difference and the dipole moment matrix element decrease with the electric field. Figure 6b exhibits the variation of the energy transition and dipole moment matrix element as a function of the applied magnetic field. The magnetic field gives parabolic effects on the QW structure and the interband transition energy increases while the dipole moment matrix element decreases [44]. In Fig. 6c, the intense laser field is turned on. The width of the potential well reduces and the interband transition energy increases as a function of the applied *ILF* due to the shift of the conduction band toward the larger values of energy with the influence of *ILF*.

Fig. 5 Interband energy transition and dipole moment matrix elements for different structure parameters **a** with A and **b** with M
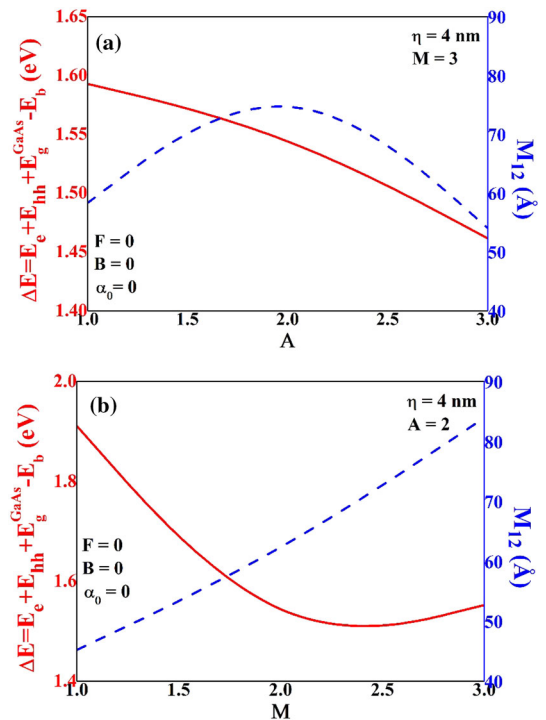

Fig. 6 Interband energy transition and dipole moment matrix elements for different applied external fields; **a** electric field **b** magnetic field and **c** intense laser field
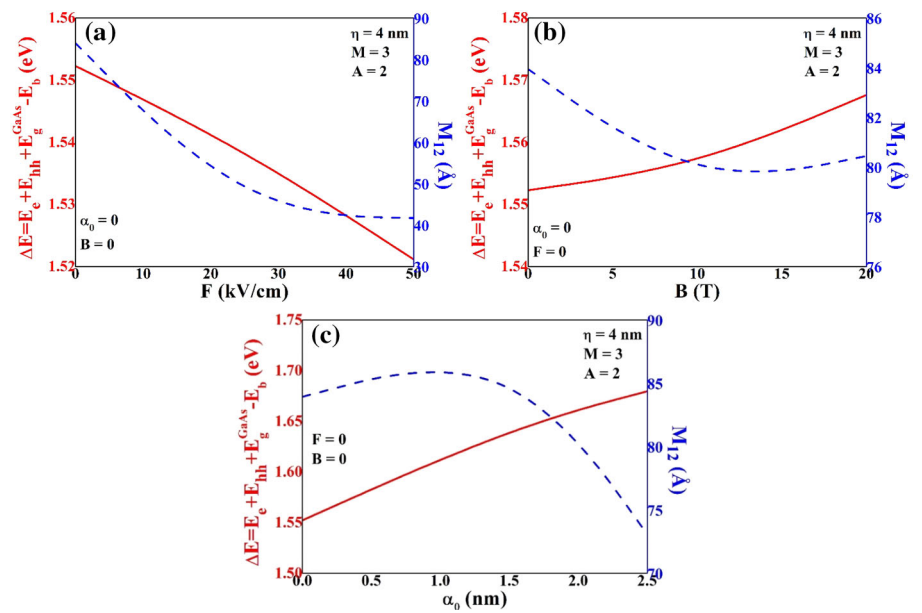

Figure 7 contains the results for total optical absorption coefficients (TOAC) related to the interband transition between the ground state electron and heavy hole for different dimensionless parameters (a) A and (b) M. The resonant peak of TOAC is obtained as a function of incident photon energy for different A parameters as shown in Fig. 7a. The TOAC peak position shifts to a lower energy region with the increment of A. The potential shape turns from double QW to single QW with the increment of A parameters. The energy difference between the ground state electron and heavy hole decreases with the increment of A. The amplitude of the TOAC peak increases first and then decreases with the increment of A. This variation of the TOAC peak is explained by the behavior of the interband transition energies as shown in Fig. 5a. Figure 7b exhibits the change of the TOAC resonant peak at different M parameters. The increment of M results in the decrement of the interband transition energy. There is a sharp decrease in the interband transition energy for $M = 1 \rightarrow 2$. Then $M = 2 \rightarrow 3$, the interband transition energy slightly changes. Such an internal energy variation leads to a redshift of the TOAC resonant peaks. The dipole moment matrix elements mainly affect the amplitude of the resonant TOAC peaks.

Fig. 7 Total optical absorption coefficient for different structure parameters of **a** A and **b** M
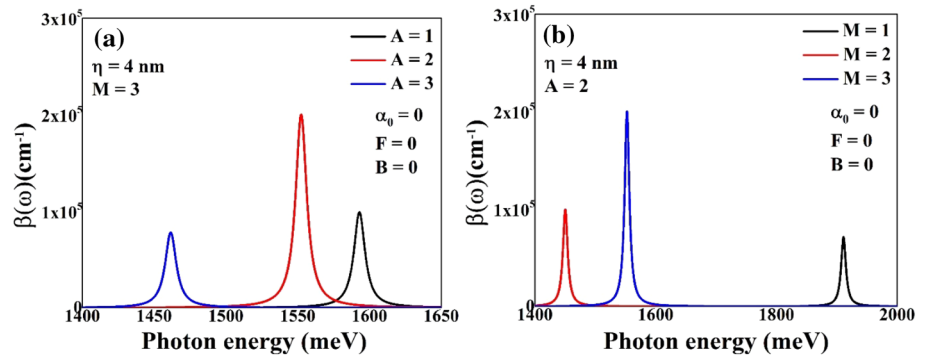

Fig. 8 Total optical absorption coefficients for different applied external fields; **a** electric field **b** magnetic field and **c** intense laser field
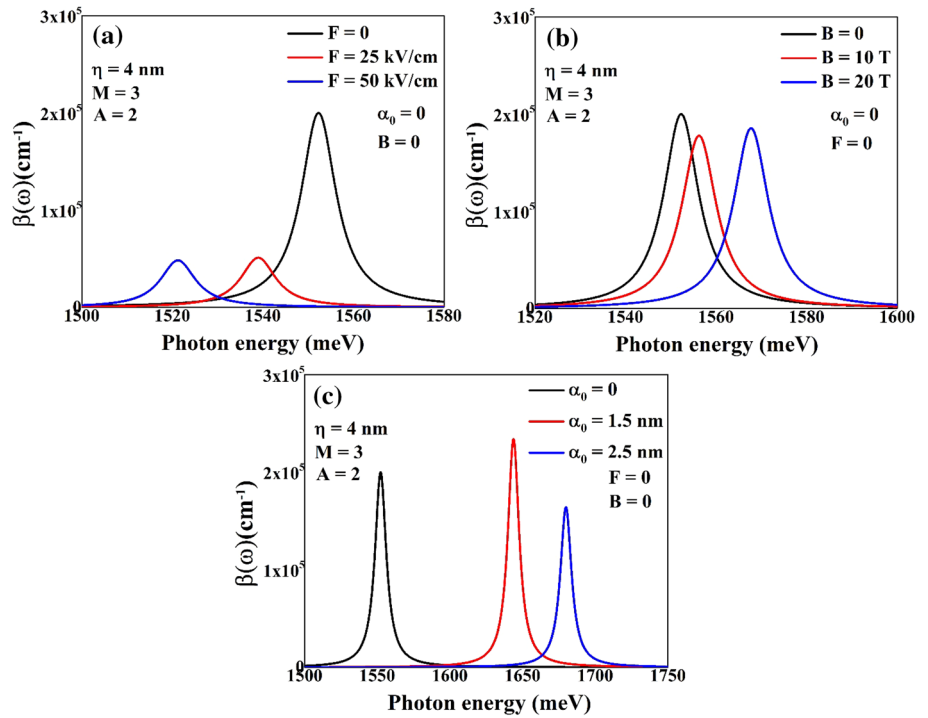

Figure 8 exhibits TOAC coefficients as a function of incident photon energy for three different applied external fields. An increment of the applied electric field results in the redshift of the TOAC peak positions as shown in Fig. 8a. The amplitude of the peaks decreases with the increment of the applied external field. The variation of the interband transition energy and the dipole moment matrix elements is seen in Fig. 6a. In Fig. 8b, the applied magnetic field moves toward the higher energy region of the TOAC peak. The amplitude of the peak slightly changes with the applied magnetic field. The applied magnetic field brings a parabolic effect on the structure. The interband transition energy and the dipole moment matrix element variation are given in Fig. 6b. When the *ILF* is turned on, the TOAC peak shifts to higher energies (blue shift) as shown in Fig. 8c. The *ILF* narrows the potential width. The ground and the first excited state energy difference increases with the applied *ILF* [45]. The effects of the *ILF* on the interband transition energy and the dipole moment matrix elements are demonstrated in Fig. 6c. The changes in the optical properties occur owing to the increase in spacing energy between the energy levels. The performed numerical results are useful to determine the effects of the structural parameters and the applied external fields on the TOACs of the Razavy QW structure.

4 Conclusion

In this study, we have performed a numerical simulation to obtain the effect of the quantum-well parameters and the applied external fields on the total optical absorption coefficients. The ground state electron and heavy hole interband electronic transition of GaAs quantum well having Razavy confinement potential shape and electronic wavefunctions have been calculated using the diagonalization method. The obtained numerical results demonstrate that the Razavy potential profile turns into a single quantum-well structure for particular dimensionless structure parameters, using Razavy potential parameters, the quantum-well system evolves

from the double quantum well to a single quantum well and the resonant peak position is sensitive to the structure parameters and the applied external fields. The variation of these physical quantities shifts resonant peaks toward lower and higher energies as well as the relative change in their amplitudes. The control of these parameters tunes the optical and electronic properties of the GaAs quantum well with Razavy confinement potential.

Data Availability Statement The corresponding author will provide the files in case they are requested. This manuscript has associated data in a data repository. [Authors' comment: The data would be available upon request.]

Declaration

Conflict of interest The authors declare that they have no known competing financial interests or personal relationships that could have appeared to influence the work reported in this paper.

References

1. R.L. Restrepo, J.P. González-Pereira, E. Kasapoglu, A.L. Morales, C.A. Duque, Linear and nonlinear optical properties in the terahertz regime for multiple-step quantum wells under intense laser field: electric and magnetic field effects. Opt. Mater. **86**, 590–599 (2018)
2. E.C. Niculescu, Electromagnetically induced transparency in an asymmetric double quantum well under non-resonant, intense laser fields. Opt. Mater. **64**, 540–547 (2017)
3. H.V. Phuc, N. Duy Anh Tuan, L. Dinh, Linear and nonlinear magneto-optical absorption in a quantum well modulated by intense laser field. Superlattices Microstruct. **100**, 1112–1119 (2016)
4. J.-F. You, Q. Zhao, Z.-H. Zhang, J.-H. Yuan, K.-X. Guo, E. Feddi, The effect of temperature, hydrostatic pressure and magnetic field on the nonlinear optical properties of AlGaAs/GaAs semi-parabolic quantum well. Int. J. Mod. Phys. B **33**, 1950325 (2019)
5. H.M. Youssef, A.A. El-Bary, Generalized thermoelastic infinite layer subjected to ramp-type thermal and mechanical loading under three theories—state space approach. J. Therm. Stresses **32**, 1293–1309 (2009)
6. M.A. Ezzat, A.A. El-Bary, Magneto-thermoelectric viscoelastic materials with memory-dependent derivative involving two-temperature. Int. J. Appl. Electromagn. Mech. **50**, 549–567 (2016)
7. M. Ezzat, A.A. El-Bary, S. Ezzat, Combined heat and mass transfer for unsteady MHD flow of perfect conducting micropolar fluid with thermal relaxation. Energy Convers. Manage. **52**, 934–945 (2011)
8. G. Liu, K. Guo, Z. Zhang, H. Hassanbadi, L. Lu, Electric field effects on nonlinear optical rectification in symmetric coupled AlxGa1−xAs/GaAs quantum wells. Thin Solid Films **662**, 27–32 (2018)
9. G. Liu, K. Guo, H. Hassanabadi, L. Lu, Linear and nonlinear optical properties in a disk-shaped quantum dot with a parabolic potential plus a hyperbolic potential in a static magnetic field. Physica B **407**, 3676–3682 (2012)
10. A. Ghanbari, R. Khordad, F. Taghizadeh, Influence of Coulomb term on thermal properties of fluorine. Chem. Phys. Lett. **801**, 139725 (2022)
11. B.O. Alaydin, D. Altun, E. Ozturk, Linear and nonlinear optical properties of semi-elliptical InAs quantum dots: effects of wetting layer thickness and electric field. Thin Solid Films **755**, 139322 (2022)
12. M. Sayrac, A. Turkoglu, F. Ungan, Influence of hydrostatic pressure, temperature, and terahertz laser field on the electron-related optical responses in an asymmetric double quantum well. Eur Phys J B **94**, 121 (2021)
13. M. Sayrac, Effects of applied external fields on the nonlinear optical rectification, second, and third-harmonic generation in an asymmetrical semi exponential quantum well. Opt. Quant. Electron. **54**, 52 (2021)
14. I. Karabulut, E. Paspalakis, The role of permanent dipoles on the intensity-dependent nonlinear optical properties in asymmetric coupled quantum wells under a static electric field. Physica E **81**, 294–301 (2016)
15. K. Li, K. Guo, X. Jiang, M. Hu, Effect of position-dependent effective mass on nonlinear optical properties in a quantum well. Optik **132**, 375–381 (2017)
16. B.T. Diroll, M. Chen, I. Coropceanu, K.R. Williams, D.V. Talapin, P. Guyot-Sionnest, R.D. Schaller, Polarized near-infrared intersubband absorptions in CdSe colloidal quantum wells. Nat. Commun. **10**, 4511 (2019)
17. H. Dakhlaoui, M. Nefzi, Simultaneous effect of impurities, hydrostatic pressure, and applied potential on the optical absorptions in a GaAs field-effect transistor. Results Phys. **15**, 102618 (2019)
18. H. Noverola-Gamas, L.M. Gaggero-Sager, O. Oubram, Interlayer distance effects on absorption coefficient and refraction index change in p-type double-δ-doped GaAs quantum wells*. Chin. Phys. B **28**, 124207 (2019)
19. H. Yıldırım, Many-body effects on intersubband transitions in polar ZnO/ZnMgO multiple quantum wells. Physica B **571**, 26–31 (2019)
20. M.A. Ezzat, A.S. El-Karamany, A.A. El-Bary, M.A. Fayik, Fractional ultrafast laser-induced magneto-thermoelastic behavior in perfect conducting metal films. J. Electromagn. Waves Appl. **28**, 64–82 (2014)
21. G. Liu, K. Guo, Z. Zhang, H. Hassanbadi, L. Lu, Nonlinear optical rectification in laterally-coupled quantum well wires with applied electric field. Superlattices Microstruct. **103**, 230–244 (2017)
22. W. Zhai, H. Hassanbadi, L. Lu, G. Liu, A theoretical study of third-harmonic generation in semi-parabolic plus semi-inverse squared quantum wells. Opt. Commun. **319**, 95–99 (2014)
23. B.O. Alaydin, Effect of high bandgap AlAs quantum barrier on electronic and optical properties of In0.70Ga0.30As/Al0.60In0.40As superlattice under applied electric field for laser and detector applications. Int. J. Modern Phys. B **35**, 2150027 (2021)
24. M. Sayrac, A. Turkoglu, M.E. Mora-Ramos, F. Ungan, Intensity-dependent nonlinear optical properties in an asymmetric Gaussian potential quantum well-modulated by external fields. Opt. Quant. Electron. **53**, 485 (2021)
25. H. Dakhlaoui, M. Nefzi, Tuning the linear and nonlinear optical properties in double and triple δ—doped GaAs semiconductor: Impact of electric and magnetic fields. Superlattices Microstruct. **136**, 106292 (2019)
26. F. Ungan, M.K. Bahar, J.C. Martinez-Orozco, M.E. Mora-Ramos, Optical responses in asymmetric hyperbolic-type quantum wells under the effect of external electromagnetic fields. Photonics Nanostruct. Fundam. Appl. **41**, 100833 (2020)
27. N.D. Hien, C.A. Duque, E. Feddi, N.V. Hieu, H.D. Trien, L.T.T. Phuong, B.D. Hoi, L.T. Hoa, C.V. Nguyen, N.N. Hieu, H.V. Phuc, Magneto-optical effect in GaAs/GaAlAs semi-parabolic quantum well. Thin Solid Films **682**, 10–17 (2019)
28. E.F. Schubert, Delta doping of III–V compound semiconductors: Fundamentals and device applications. J. Vac. Sci. Technol. A **8**, 2980–2996 (1990)

29. K. Ploog, M. Hauser, A. Fischer, Fundamental studies and device application of δ-doping in GaAs Layers and in AlxGa1−xAs/GaAs heterostructures. Appl. Phys. A **45**, 233–244 (1988)
30. A.C. Maciel, M. Tatham, J.F. Ryan, J.M. Worlock, R.E. Nahory, J.P. Harbison, L.T. Florez, Raman scattering from electronic excitations in periodically δ-doped GaAs. Surf. Sci. **228**, 251–254 (1990)
31. M.H. Degani, Electron energy levels in a delta doped layer in GaAs. Phys. Rev. B **44**, 5580–5584 (1991)
32. G. Liu, K. Guo, H. Hassanabadi, L. Lu, B.H. Yazarloo, A theoretical study of nonlinear optical absorption and refractive index changes with the three-dimensional ring-shaped pseudoharmonic potential. Physica B **415**, 92–96 (2013)
33. L. Lu, W. Xie, H. Hassanabadi, Linear and nonlinear optical absorption coefficients and refractive index changes in a two-electron quantum dot. J. Appl. Phys. **109**, 063108 (2011)
34. L. Lu, W. Xie, H. Hassanabadi, The effects of intense laser on nonlinear properties of shallow donor impurities in quantum dots with the Woods-Saxon potential. J. Lumin. **131**, 2538–2543 (2011)
35. H.R. Rastegar Sedehi, R. Khordad, H. Bahramiyan, Optical properties and diamagnetic susceptibility of a hexagonal quantum dot: impurity effect. Opt. Quantum Electron. **53**, 264 (2021)
36. H.S. Aydinoglu, M. Sayrac, M.E. Mora-Ramos, F. Ungan, Nonlinear optical properties in AlxGa1-xAs/GaAs double-graded quantum wells: The effect of the structure parameter, static electric, and magnetic field. Solid State Commun. **342**, 114647 (2022)
37. J. Osvald, Electronic properties of a near surface Si -doped GaAs under an applied electric field. J. Phys. D Appl. Phys. **37**, 2655–2659 (2004)
38. K.M. Wong, D.W.E. Allsopp, Intersubband absorption modulation in coupled double quantum wells by external bias. Semicond. Sci. Technol. **24**, 045018 (2009)
39. H. Hassanabadi, G. Liu, L. Lu, Nonlinear optical rectification and the second-harmonic generation in semi-parabolic and semi-inverse squared quantum wells. Solid State Commun. **152**, 1761–1766 (2012)
40. H. Hassanabadi, H. Rahimov, L. Lu, C. Wang, Nonlinear optical properties of a three-electron quantum dot with account of the Rashba spin–orbit interaction. J. Lumin. **132**, 1095–1100 (2012)
41. J. Krupski, M. Piętka, On the accuracy of the Thomas-Fermi-Dirac method applied to sub-band structure calculations in a δ-doped semiconductor. Solid State Commun. **107**, 141–144 (1998)
42. E. Ozturk, Y. Ergun, H. Sari, I. Sokmen, The self-consistent calculation of Si δ-doped GaAs structures. Appl. Phys. A **73**, 749–754 (2001)
43. E. Kasapoglu, F. Ungan, H. Sari, I. Sökmen, The hydrostatic pressure and temperature effects on donor impurities in cylindrical quantum wire under the magnetic field. Physica E **42**, 1623–1626 (2010)
44. R. Khordad, S.K. Khaneghah, M. Masoumi, Effect of pressure on intersubband optical absorption coefficients and refractive index changes in a V-groove quantum wire. Superlattices Microstruct. **47**, 538–549 (2010)
45. L. Lu, W. Xie, H. Hassanabadi, Laser field effect on the nonlinear optical properties of donor impurities in quantum dots with Gaussian potential. Physica B **406**, 4129–4134 (2011)
46. L.M. Gaggero-Sager, G.G. Naumis, M.A. Muñoz-Hernandez, V. Montiel-Palma, Self-consistent calculation of transport properties in Si δ-doped GaAs quantum wells as a function of the temperature. Physica B **405**, 4267–4270 (2010)
47. R.B. Dhafer, H. Saidi, S. Ridene, Proposal of InP/AlInGaAs single delta quantum well for fiber-optic communications. Optik **158**, 164–169 (2018)
48. M. Razavy, An exactly soluble Schrödinger equation with a bistable potential. Am. J. Phys. **48**, 285–288 (1980)
49. M. Baradaran, H. Panahi, Exact solutions of a class of double-well potentials: algebraic bethe ansatz. Adv. High Energy Phys. **2017**, 8429863 (2017)
50. H. Karayer, D. Demirhan, K.G. Atman, Analytical exact solutions for the Razavy type potential. Math. Methods Appl. Sci. **43**, 9185–9194 (2020)
51. E. Kasapoglu, H. Sari, I. Sökmen, J.A. Vinasco, D. Laroze, C.A. Duque, Effects of intense laser field and position dependent effective mass in Razavy quantum wells and quantum dots. Physica E **126**, 114461 (2021)
52. V.K. Arora, Quantum size effect in thin-wire transport. Phys. Rev. B **23**, 5611–5612 (1981)
53. J. Lee, H.N. Spector, Hydrogenic impurity states in a quantum well wire. J. Vacuum Sci. Technol. B Microelectron. Process. Phenomena **2**, 16–20 (1984)
54. S. Luryi, F. Capasso, Resonant tunneling of two-dimensional electrons through a quantum wire: a negative transconductance device. Appl. Phys. Lett. **47**, 1347–1349 (1985)
55. E.C. Garnett, M.L. Brongersma, Y. Cui, M.D. McGehee, Nanowire solar cells. Annu. Rev. Mater. Res. **41**, 269–295 (2011)
56. F. Zaouali, A. Bouazra, M. Said, A theoretical evaluation of optical properties of InAs/InP quantum wire with a dome cross-section. Optik **174**, 513–520 (2018)
57. L. Van-Tan, T.V. Thang, N.D. Vy, H.T. Cao, Spin polarization and temperature dependence of electron effective mass in quantum wires. Phys. Lett. A **383**, 2110–2113 (2019)
58. P. Hosseinpour, Effect of Gaussian impurity parameters on the valence and conduction subbands and thermodynamic quantities in a doped quantum wire. Solid State Commun. **322**, 114061 (2020)
59. E. Kasapoglu, I. Sökmen, Interband absorption and exciton binding energy in an inverse parabolic quantum well under the magnetic field. Phys. Lett. A **372**, 56–59 (2007)
60. F.M.S. Lima, O.A.C. Nunes, M.A. Amato, A.L.A. Fonseca, E.F. da Silva Jr, Dichotomy of the exciton wave function in semiconductors under intense laser fields. J. Appl. Phys. **103**, 113112 (2008)
61. S. Panda, T. Das, B.K. Panda, Nonlinear optical susceptibilities in InxGa1−xN/GaN hexagonal single quantum well under applied electric field. Superlattices Microstruct. **135**, 106238 (2019)
62. Z.-H. Zhang, K.-X. Guo, J.-H. Yuan, Influence of the position dependent effective mass on the nonlinear optical properties in semiparabolic and parabolic quantum well with applied magnetic field. Physica E **108**, 238–243 (2019)
63. A. Keshavarz, M.J. Karimi, Linear and nonlinear intersubband optical absorption in symmetric double semi-parabolic quantum wells. Phys. Lett. A **374**, 2675–2680 (2010)